DOI: 10.1002/chem.200500865

Preferred 3D-Structure of Peptides Rich in a Severely Conformationally Restricted Cyclopropane Analogue of Phenylalanine

Marco Crisma,[a] Wim M. De Borggraeve,[a] Cristina Peggion,[a] Fernando Formaggio,[a] Soledad Royo,[b] Ana I. Jiménez,[b] Carlos Cativiela,[b] and Claudio Toniolo*[a]

Abstract: Terminally blocked, homopeptide amides of (*R*,*R*)-1-amino-2,3-diphenylcyclopropane-1-carboxylic acid ($c_3$diPhe), a chiral member of the family of C^α-tetrasubstituted α-amino acids, from the dimer to the tetramer, and diastereomeric co-oligopeptides of (*R*,*R*)- or (*S*,*S*)-$c_3$diPhe with (*S*)-alanine residues to the trimer level were prepared in solution and fully characterized. The synthetic effort was extended to terminally protected co-oligopeptide esters to the hexamer, where $c_3$diPhe residues are combined with achiral α-aminoisobutyric acid residues. The preferred conformations of the peptides were assessed in solution by FT-IR absorption, NMR, and CD techniques, and for seven oligomers in the crystal state (by X-ray diffraction) as well. This study clearly indicates that $c_3$diPhe, a sterically demanding cyclopropane analogue of phenylalanine, tends to fold peptides into β-turn and 3_{10}-helix conformations. However, when $c_3$diPhe is in combination with other chiral residues, the conformation preferred by the resulting peptides is also dictated by the chiral sequence of the amino acid building blocks. The (*S*,*S*)-enantiomer of this α-amino acid, unusually lacking asymmetry in the main chain, strongly favors the left-handedness of the turn/helical peptides formed.

Keywords: chirality · conformation analysis · NMR spectroscopy · peptides · X-ray diffraction

Introduction

Insertion of non-protein, C^α-tetrasubstituted α-amino acids into peptides dramatically reduces the available conformational space by stabilizing specific secondary structures,[1,2] such as β-[3–5] and γ-[4,6,7] turns, 3_{10}- and α-helices,[8,9] and the fully-extended structure.[4,9] Furthermore, these backbone-modified peptides become more resistant to proteases. It was suggested that peptides rich in C^α-tetrasubstituted α-amino acids may represent unique foldamers[10] and be exploited as useful, conformationally constrained, molecular bridges or scaffolds in supramolecular chemistry, spectroscopy, electrochemistry, and catalyzed asymmetric synthesis.[9,11]

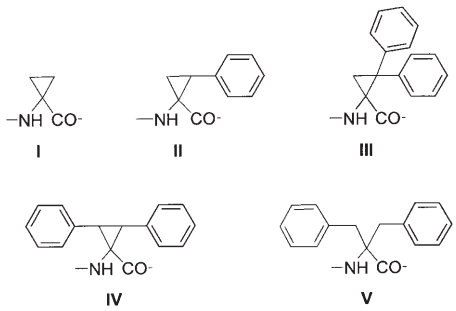

The preferred conformations of the prototypical Ac_3c (1-aminocyclopropane-1-carboxylic acid or 2,3-methanoalanine) residue (**I**)[2,12–14] and its mono- (**II**)[15–18] and di- (**III**)[19–21] phenyl side-chain substituted congeners were evaluated in solution as well as in the crystal state and found to be strongly biased towards the β-/γ-turn and related helical conformations. Interestingly enough, a terminally-blocked

[a] Dr. M. Crisma, Dr. W. M. De Borggraeve, Dr. C. Peggion, Prof. F. Formaggio, Prof. C. Toniolo
Institute of Biomolecular Chemistry, CNR
Department of Chemistry, University of Padova
via Marzolo 1, 35131 Padova (Italy)
Fax: (+39) 049-827-5239
E-mail: claudio.toniolo@unipd.it

[b] S. Royo, Dr. A. I. Jiménez, Prof. C. Cativiela
Department of Organic Chemistry, ICMA
University of Zaragoza - CSIC
50009 Zaragoza (Spain)

Supporting information for this article is available on the WWW under http://www.chemeurj.org/ or from the author.

dipeptide characterized by residue **III** at position 2 was recently found to fold in the unusual, incipient 2.2_7-helix (two consecutive γ-turns).[21]

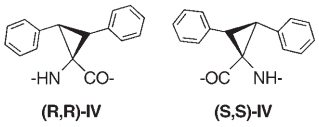

(R,R)-IV (S,S)-IV

To complete our understanding of the 3D-structural propensities of the phenyl-substituted, $C^{\alpha}\leftrightarrow C^{\alpha}$-cyclized, cyclopropane α-amino acids and to offer new tools to peptide chemists for the control of conformation, we embarked on a program directed towards an in-depth 3D-structural characterization of peptides rich in either the (*R*,*R*)- or the (*S*,*S*)-enantiomer of $c_3$diPhe (**IV**, 1-amino-*c*-2,*t*-3-diphenylcyclopropane-*r*-1-carboxylic acid). This residue may be considered as derived from $C^{\alpha,\alpha}$-dibenzylglycine (**V**)[2] through a formal C^{β}–$C^{\beta'}$ covalent bond formation (cyclopropanation). The stereochemical properties of this α-amino acid are peculiar in that it bears two phenyl substituents on adjacent side-chain β-carbons in a *trans* relative disposition and is therefore characterized by an achiral α-carbon and two chiral β-carbons, with two enantiomeric forms being possible, (*R*,*R*) and (*S*,*S*).

The few published articles containing conformational data on $c_3$diPhe derivatives and peptides as short as dipeptides[20,22–24] seem to indicate that this residue tends to fall in the helical regions [A and A*] of the ϕ,ψ space.[25] However, these compounds are either too short to form any commonly found H-bonded folded structure (amino acid derivatives) or they are preceded in the sequence by a Pro residue, which is known to possess by itself a strong conformational bias.[26,27] Interestingly, a single (*R*,*R*)-$c_3$diPhe residue, positioned in the middle of an N- and C-blocked, all-*S*, 13-mer peptide, was shown to enforce helicity.[28] Conversely, (*S*,*S*)-$c_3$diPhe precludes helicity in the diastereomeric peptide.

In particular, in this paper we describe the synthesis and chemical characterization of a variety of terminally-blocked $c_3$diPhe model peptides. These include a homo-chiral, homo-oligomeric $c_3$diPhe series (to the tetramer level) and co-oligopeptides in which $c_3$diPhe is combined with the achiral residue α-aminoisobutyric acid (Aib) (to the hexamer) or with the chiral residue (*S*)-Ala (to the trimer). In this latter case diastereomeric di- and tripeptides were also prepared. A detailed conformational analysis in solution (by FT-IR absorption, NMR, and CD techniques) and in the crystal state (by X-ray diffraction) of twelve carefully selected examples **1**–**12**, the sequences of which are shown and numbered in Table 1 (see below), is also reported. Aib is known to strongly stabilize turn/helical structures,[1,2] while Ala easily accommodates in turns or in extended conformations. Preliminary results of a part of this work have been reported.[29]

Results and Discussion

Synthesis and characterization: The preparation and characterization of the $c_3$diPhe derivatives Boc-(*R*,*R*)-$c_3$diPhe-OH[23] (Boc, *tert*-butyloxycarbonyl), Boc-(*S*,*S*)-$c_3$diPhe-OH,[23] and Boc-(*R*,*R*)-$c_3$diPhe-NH*i*Pr[29] (*i*Pr, isopropyl) were already reported. Peptide synthesis was performed step-by-step in solution beginning from the C-terminus. Satisfactory to excellent yields were achieved in the difficult steps of peptide bond formation involving one or two $c_3$diPhe residues. Products were obtained after a few days of reaction using the EDC (*N*-ethyl,*N*′-[3′-(dimethylamino)propyl]carbodiimide)/HOAt (7-aza-1-hydroxy-1,2,3-benzotriazole) or the HOAt/HATU {*N*-[(dimethylamino)-1*H*-1,2,3-triazolo[4,5*b*]pyridin-1-yl-methylene]-*N*-methylmethanaminium hexafluorophosphate *N*-oxide} method[30] in methylene chloride (or chloroform) solution in the presence of a tertiary amine (*N*-methylmorpholine or *N*,*N*-diisopropylethylamine). The Boc-Xxx-NHMe (NHMe, methylamino) derivatives, where Xxx is (*S*,*S*)-$c_3$diPhe, (*R*,*R*)-$c_3$diPhe or (*S*)-Ala, were synthesized via the mixed anhydride method with isobutylchloroformate and *N*-methylmorpholine. Pivaloylation was obtained by use of Piv-Cl (Piv, pivaloyl or *tert*-butylcarbonyl) in chloroform solution in the presence of *N*-methylmorpholine. The Boc group was removed by using mild acidolysis.

The physical properties and analytical data for the $c_3$diPhe derivatives and peptides are listed in Table 1. All newly synthesized compounds were also characterized by ^{1}H NMR and elemental analyses (see Supporting Information).

Solution conformational analysis: Preliminary information on the solution conformational preferences of the $c_3$diPhe rich peptides, in particular of the homo-chiral homo-peptides **10**–**12** and $c_3$diPhe/Aib co-oligopeptides **6**–**9**, was obtained in a solvent of low polarity, $CDCl_3$, by FT-IR absorption as a function of concentration (in the range 10–0.1 mM). The spectra in the informative N–H stretching region (amide A) are reported in Figure 1.

In the longest oligomers the curves are characterized by two prominent bands, at 3430–3425 cm^{-1} (free NH groups) and 3355–3320 cm^{-1} (H-bonded NH groups), respectively.[31–33] The intensity of the low-frequency band relative to that of the high-frequency band increases as the main-chain length is enhanced. Concomitantly, the absorption maximum shifts markedly to lower wavenumbers. In the shortest oligomers a band at 3415–3390 cm^{-1} of variable intensity, arising from weakly H-bonded NH groups of fully-extended conformers, is also seen. By examining the spectra at various concentrations we demonstrated that significant self-association is absent in all peptides except in the $c_3$diPhe/Aib hexamer **9** (but only above 1 mM concentration) (spectra not shown). Consequently, the observed hydrogen bonding should be interpreted as due almost exclusively to intramolecular C=O···H-N interactions.

The present FT-IR absorption study has provided clear evidence that main-chain length dependent intramolecular

Table 1. Physical properties and analytical data for the $c_3$diPhe derivatives and peptides.

Peptide	Yield [%]	M.p. [°C][a]	Recryst. solvent[b]	$[\alpha]_D^{20}$[c]	TLC[d]		
					R_f(I)	R_f(II)	R_f(III)
Boc-(*S*,*S*)-$c_3$diPhe-NHMe	95	176–177	Et_2O	−159.7[e]	0.45	0.85	0.30
Boc-(*R*,*R*)-$c_3$diPhe-NHMe	96	176–177	Et_2O	152.8[e]	0.45	0.90	0.30
Boc-(*S*,*S*)-$c_3$diPhe-(*S*)-Ala-NHMe	98	197–198	iPr_2O/CH_2Cl_2	−145.3	0.50	0.85	0.40
Boc-(*R*,*R*)-$c_3$diPhe-(*S*)-Ala-NHMe	97	186–188	iPr_2O/CH_2Cl_2	138.2	0.45	0.85	0.35
Boc-(*S*)-Ala-(*S*,*S*)-$c_3$diPhe-NHMe (**1**)	85	240–241	iPr_2O/CH_2Cl_2	−174.6	0.50	0.85	0.35
Boc-(*S*)-Ala-(*R*,*R*)-$c_3$diPhe-NHMe	85	184–185	iPr_2O/CH_2Cl_2	67.1	0.50	0.85	0.35
Boc-(*S*)-Ala-(*S*,*S*)-$c_3$diPhe-(*S*)-Ala-NHMe (**2**)	89	252–253	$EtOAc/CH_2Cl_2$	−154.2	0.40	0.90	0.30
Boc-(*S*)-Ala-(*R*,*R*)-$c_3$diPhe-(*S*)-Ala-NHMe (**3**)	71	252–254	$EtOAc/CH_2Cl_2$	116.8	0.35	0.85	0.25
Piv-(*S*,*S*)-$c_3$diPhe-(*S*)-Ala-NHMe (**4**)	97	298–299	$EtOAc/CH_2Cl_2$	−147.1[h]	0.50	0.85	0.40
Piv-(*R*,*R*)-$c_3$diPhe-(*S*)-Ala-NHMe (**5**)	99	245–246	$EtOAc/CH_2Cl_2$	149.3	0.45	0.80	0.35
Piv-(*S*)-Ala-(*S*,*S*)-$c_3$diPhe-NHMe	96	284	$iPr_2O/CHCl_3$	−173.8	0.50	0.85	0.35
Piv-(*S*)-Ala-(*R*,*R*)-$c_3$diPhe-NHMe	99	165–166	iPr_2O/CH_2Cl_2	72.4	0.45	0.85	0.35
Piv-(*S*)-Ala-(*S*,*S*)-$c_3$diPhe-(*S*)-Ala-NHMe	94	269–270	$EtOAc/CH_2Cl_2$	−160.6	0.35	0.85	0.25
Piv-(*S*)-Ala-(*R*,*R*)-$c_3$diPhe-(*S*)-Ala-NHMe	74	291–292	$EtOAc/CH_2Cl_2$	106.7	0.35	0.90	0.25
Boc-(*S*,*S*)-$c_3$diPhe-Aib-Aib-OMe (**6**)	92	155–156	EtOAc/PE	−102.2	0.85	0.90	0.45
Boc-Aib-(*S*,*S*)-$c_3$diPhe-Aib-Aib-OMe (**7**)	65	228–229	EtOAc/PE	−88.9	0.80	0.70	0.40
Boc-Aib-Aib-(*S*,*S*)-$c_3$diPhe-Aib-Aib-OMe (**8**)	70	253–254	$CHCl_3/Et_2O$	−71.0	0.70	0.85	0.30
Boc-[(*S*,*S*)-$c_3$diPhe-Aib-Aib]$_2$-OMe (**9**)	43	285–286[f]	$CHCl_3/Et_2O$	−150.9	0.75	0.90	0.35
Boc-[(*R*,*R*)-$c_3$diPhe]$_2$-NH*i*Pr (**10**)	61	196–197	Et_2O/PE	209.6	0.95	0.90	0.70
Boc-[(*R*,*R*)-$c_3$diPhe]$_3$-NH*i*Pr (**11**)	84	226–227	EtOAc/PE	290.2[g]	0.95	0.95	0.60
Boc-[(*R*,*R*)-$c_3$diPhe]$_4$-NH*i*Pr (**12**)	70	253–254[f]	EtOAc/PE	363.3	0.90	0.90	0.40

[a] Determined on a Gallenkamp (Loughborough, U.K.) apparatus and are uncorrected. [b] EtOA*c* = ethyl acetate, PE = petroleum ether, iPr_2O = diisopropyl ether. [c] Determined on a Jasco P-1020 (Tokyo, Japan) polarimeter equipped with a thermostat; $c = 0.5$ (methanol). [d] Kieselgel F-254 silica gel plates (Merck, Darmstadt, Germany) and the following solvent systems: I) chloroform/ethanol 9:1; II) butan-1-ol/acetic acid/water 3:1:1; III) toluene/ethanol 7:1; the spots were visualized by using UV light ($\lambda = 254$ nm) or through development with the hypochlorite/starch/iodide chromatic reaction as appropriate; a single spot was observed in each case. [e] $c = 0.85$ (methanol). [f] with decomposition. [g] $c = 0.1$ (methanol). [h] $c = 0.2$ (methanol).

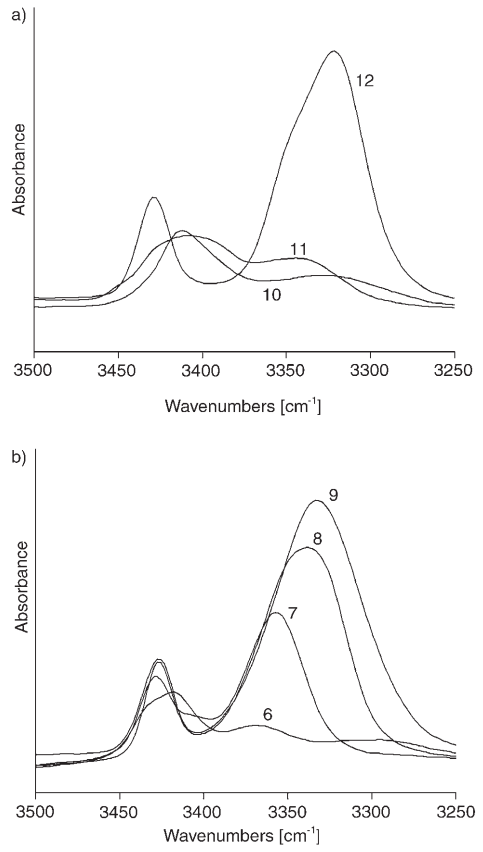

Figure 1. FT-IR absorption spectra in the 3500–3250 cm^{-1} region of a) the Boc-[(*R*,*R*)-$c_3$diPhe]$_n$-NH*i*Pr ($n = 2$–4) (**10**–**12**) homo-peptides, and b) the tri- tetra-, penta-, and hexapeptides of the Boc/OMe terminally protected, Aib/(*S*,*S*)-$c_3$diPhe **6**–**9** series in $CDCl_3$ solution (peptide conc. 1 mM).

hydrogen bonding is a relevant factor stabilizing the conformation of the terminally blocked $c_3$diPhe-based peptides in structure supporting solvents. This finding is in full agreement with those already reported for the Aib-[34] and Ac_3c[12]-rich peptides, although in both of these cases the amounts of intramolecularly H-bonded folded forms appear to be somewhat higher. However, on the basis of the FT-IR absorption analysis only, it is not safe to distinguish unambiguously among the possible types of intramolecularly H-bonded folded forms.

To obtain more detailed information on the solution preferred conformations of the terminally-blocked $c_3$diPhe-rich peptides, an NMR study was performed. The delineation of inaccessible (or intramolecularly H-bonded) NH groups was carried out by evaluation of the temperature dependence of NH proton chemical shifts in [D_6]DMSO (dimethylsulfoxide) solution[35] [the usual titrations of NH proton chemical shifts by adding [D_6]DMSO or TEMPO (2,2,6,6-tetramethyl-1-piperidinyloxy) to a $CDCl_3$ solution could not be successfully performed with the $c_3$diPhe peptides because for each compound a relevant fraction of the NH proton signals is not visible in this halohydrocarbon due to overlapping with the $c_3$diPhe aromatic CH protons]. Figure 2 shows the behavior of the longest oligomers of the $c_3$diPhe homochiral homo-peptide and the $c_3$diPhe/Aib co-oligopeptide series (**12** and **9**, respectively). For both peptides the combined analysis of TOCSY and NOESY 2D-NMR spectra[36] led to the complete assignment of all NH proton resonances. It is evident that the chemical shifts of only two protons, NH1 and NH2, in each peptide are remarkably sensitive to

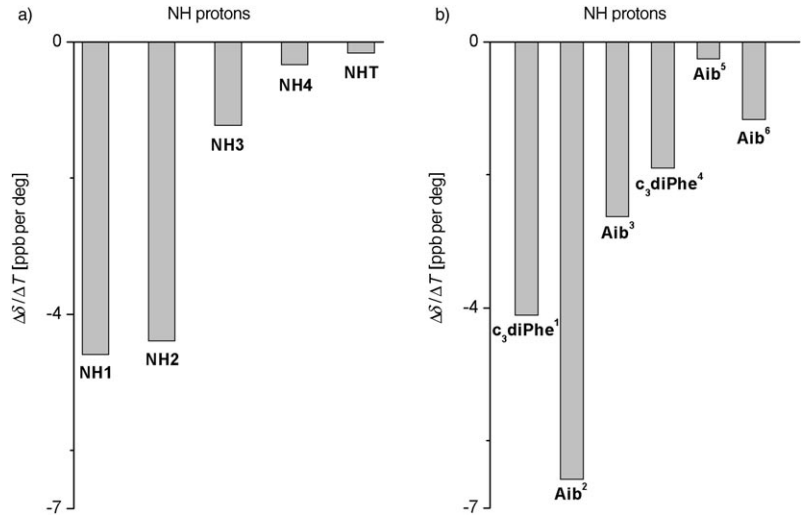

Figure 2. Plot of the variations of NH proton chemical shifts in the ^{1}H NMR spectra of a) **12** and b) **9** as a function of increasing temperature (from 25 to 60 °C) in [D_6]DMSO solution.

heating. These findings are consistent with the conclusion that even in this strong H-bonding acceptor solvent[37] the two $c_3$diPhe-rich peptides are still overwhelmingly intramolecularly H-bonded. Specifically, this is precisely the classic signature of the 3_{10}-helix.[12,34,35] The observation that the separation of the amide NH protons into this simple bimodal temperature sensitive pattern persists over the entire temperature range is a clear indication that the 3_{10}-helical hydrogen-bonding scheme is preserved up to 60 °C.

Our 2D-NMR analysis in [D_6]DMSO solution additionally suggests that the Boc-[(*R*,*R*)-$c_3$diPhe]$_4$-NH*i*Pr homo-chiral homo-tetrapeptide **12** adopts a right-handed 3_{10}-helical conformation. The ROESY ^{1}H NMR spectrum shows a complete set of $d_{NN}(i,i+1)$ NOE cross-peaks indicative of a helical structure (Figure 3a). The presence of an NOE between a C$^\beta$H proton of residue 1 and the NH proton of residue 4 (not shown), confirms that the most populated helix is of the 3_{10}-type. The right-handedness of the helix (Figure 4a) was deduced from the observation of an NOE cross-peak between the same C$^\beta$H proton of residue 1 and a C$^\beta$H proton of residue 4 (Figure 3b). In the left-handed 3_{10}-helical conformation steric repulsion between side-chain phenyl groups of residues 1 and 4 disfavors a close contact between these two C$^\beta$H protons (Figure 4b).

Although the $c_3$diPhe-based peptides studied in this work are short and rich in aromatic chromophores, we decided to investigate three relevant examples by CD spectroscopy. In methanol solution in the near-UV region (above 250 nm) the CD spectra of the Aib/(*S*,*S*)-$c_3$diPhe pentapeptide **8** (used as a "blank" as it contains only one aromatic amino acid), the Aib/(*S*,*S*)-$c_3$diPhe hexapeptide **9** (with two $c_3$diPhe residues), and the (*R*,*R*)-$c_3$diPhe homo-tetrapeptide **12** (with four such residues) all exhibit a vibrational structure (Figure 5a) typical of benzene-derived chromophores ($^1B_{2u} \leftarrow {}^1A_{1g}$ transition).[38,39] In general, these bands are remarkably more intense than those of Phe derivatives and homo-peptides,[38,39] presumably because of the considerably more restricted mobility of the aromatic chromophores in the cyclopropane-based $c_3$diPhe residues (in any case, it is worth pointing out that, in contrast to Phe, each $c_3$diPhe residue is characterized by two phenyl-substituted chromophores). As expected, the intensities of these bands for peptide **9** are approximately double than those of peptide **8**. However, this linear response is not shown by the homo-peptide **12** where intensities about ten times higher than those of the "blank" **8** are seen. This latter observation might indicate for peptide **12** a further restriction of mobility of the $c_3$diPhe side chains and/or some interaction among them. In any case, the linear response exhibited by hexapeptide **9** does not suggest per se a lack of ordered secondary structure, but simply an absence of further side-chain conformational constraints and interresidue aromatic···aromatic separations too large for productive chromophoric interactions. The sign reversal of the CD bands observed for peptide **12** is obviously assigned to the opposite chiralities of its constituent $c_3$diPhe residues.

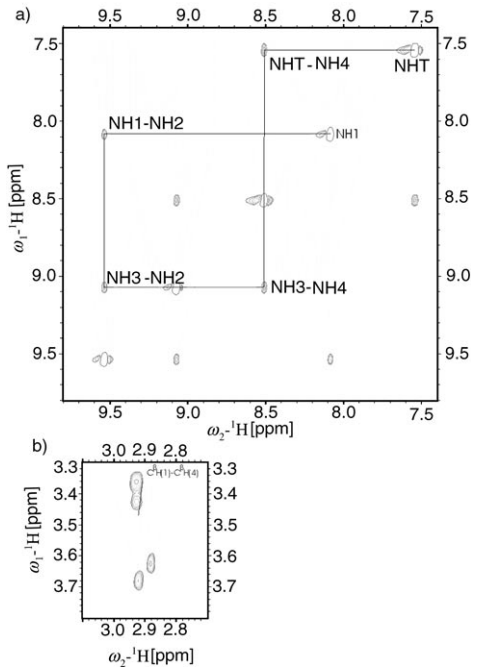

Figure 3. Sections of the ROESY spectrum of **12** in [D_6]DMSO solution a) NH region and b) C$^\beta$H region.

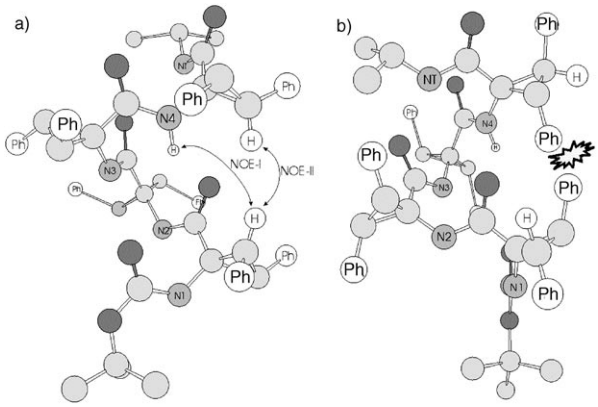

Figure 4. Computer models of a) the right-handed and b) the left-handed 3_{10}-helix of **4**.

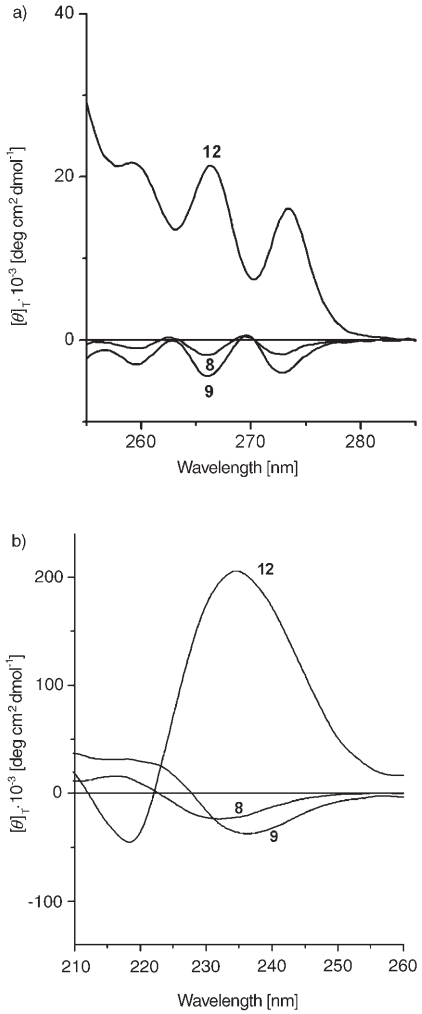

Figure 5. CD spectra of **8**, **9**, and **12** in MeOH solution in the a) near-UV and b) far-UV regions (peptide conc. 1 mM).

In the far-UV region the CD spectrum of each peptide examined exhibits oppositely signed bands, centered near 235 and 217–218 nm, respectively (Figure 5b). These curves do not correspond to any of the CD spectra typical of ordered conformations of non-aromatic peptides. Indeed, this problem is complicated by the contribution to CD of the mono-alkylated benzene side-chain chromophores which overlaps that of peptide main-chain chromophores.[39] However, the much more intense CD bands shown by the homo-tetramer **12** are clearly indicative of effective aromatic···aromatic and/or aromatic···amide interactions that can be operative only in the presence of a highly ordered conformation.

Crystal-state conformational analysis: We were able to grow single crystals amenable for an X-ray diffraction analysis from the following seven $c_3$diPhe di-, tri-, and hexapeptides: **10**, with three independent molecules (**A**, **B**, and **C**) in the asymmetric unit, **4**, **5**, **1**, **2**, **3**, and **9**. The corresponding molecular structures with atom numberings are illustrated in Figures 6–12. Table 2 lists the relevant backbone torsion angles ϕ_i, ψ_i, ω_i.[40] Tables of intra- and intermolecular H-bond parameters and of crystallographic data and structure refinements may be found in the Supporting Information (Tables S1 and S2, respectively). Despite numerous attempts, we were unable to grow any good single crystal from neither **11** nor **12**. In particular, crystals of the homo-tetrapeptide **12** were actually grown from acetonitrile solution, but they turned out to be twinned.

All thirteen $c_3$diPhe residues examined are right- or left-handed helical, the ranges of their backbone ϕ and ψ angles being rather narrow: ϕ from $\pm$72.1(6) to $\pm$50.4(7)°, ψ from $\pm$41.2(6) to $\pm$16.1(4)°.

All three molecules of the (*R*,*R*)-$c_3$diPhe homo-dipeptide **10** are conformationally similar and folded in a right-handed, slightly distorted, type-III β-turn, that is, one loop of a 3_{10}-helix (Figure 6). This conformation is stabilized by an 1←4 intramolecular (C_0=O_0···H-N_T) H-bond of moderate strength, the N···O distances being in the range from 2.987(6) to 3.004(6) Å.[41]

The 3D-structures of the two diastereomeric $c_3$diPhe-Ala dipeptides **4** and **5** are remarkably different (Figures 7 and 8). Although all four residues are helical, the (*S*,*S*)-(*S*) sequence **4** generates an overall S-shaped conformation, while the (*R*,*R*)-(*S*) sequence **5** produces a β-turn, intermediate between type-I and type-III, this latter folded structure presenting a strong intramolecular C_0=O_0···H-N_T H-bond [the N_T···O_0 distance is 2.824(4) Å]. The distinct behavior of the two diastereomeric dipeptides is associated with the observation that the (*S*,*S*)-$c_3$diPhe residue is left-handed helical whereas the (*R*,*R*)-$c_3$diPhe residue is right-handed helical, and that these conformational propensities are combined with the usual right-handed helical tendency of (*S*)-Ala.

Conversely, the (*S*)-Ala-(*S*,*S*)-$c_3$diPhe dipeptide **1** is folded in a (slightly distorted) type-II β-turn conformation, further characterized by a weak intramolecular C_0=O_0···H-N_T H-bond [the N_T···O_0 distance is 3.101(3) Å], again confirming the bias of the (distorted) helical (*S*,*S*)-$c_3$diPhe residue for the left-handed screw sense (Figure 9).

A comparison of the two diastereomeric Ala-$c_3$diPhe-Ala tripeptides **2** and **3** additionally confirms the relevant role played by the sequence chirality. In the (*S*)-(*S*,*S*)-(*S*) tripep-

Table 2. Relevant backbone torsion angles [°] for the seven $c_3$diPhe peptide structures solved in this work.

Torsion angle	(R,R)-$c_3$diPhe homo-dipeptide			(S,S)-$c_3$diPhe-(S)-Ala dipeptide	(R,R)-$c_3$diPhe-(S)-Ala dipeptide	(S)-Ala-(S,S)-$c_3$diPhe dipeptide	(S)-Ala-(S,S)-$c_3$diPhe-(S)-Ala tripeptide	(S)-Ala-(R,R)-$c_3$diPhe-(S)-Ala tripeptide	Aib/(S,S)-$c_3$diPhe hexapeptide
	10			**4**	**5**	**1**	**2**	**3**	**9**
	A	**B**	**C**						
θ^1	172.2(4)	−178.3(5)	179.7(6)			168.7(3)	−172.3(5)	−160.2(3)	177.8(6)
ω_o	−159.4(4)	−169.7(4)	−160.1(5)	178.8(2)	−172.1(3)	−177.9(3)	169.9(5)	−179.9(3)	168.1(5)
φ_1	−72.0(6)	−67.1(6)	−72.1(6)	57.3(3)	−64.9(4)	−56.9(4)	−67.3(7)	−55.3(4)	64.5(7)
ψ_1	−22.9(7)	−22.2(7)	−17.6(7)	39.2(3)	−25.8(4)	134.6(2)	147.8(5)	−30.6(4)	28.8(8)
ω_1	168.8(4)	173.2(5)	167.6(5)	−167.1(2)	172.1(3)	177.4(2)	169.6(5)	177.7(3)	−176.5(5)
φ_2	−50.4(7)	−53.4(7)	−53.1(7)	−92.8(3)	−82.6(3)	68.5(3)	63.8(7)	−58.0(4)	49.3(8)
ψ_2	−35.9(7)	−41.2(6)	−31.9(7)	−31.2(3)	−14.4(5)	20.1(4)	31.2(8)	−16.1(4)	34.8(7)
ω_2	−173.1(6)	169.8(5)	−177.6(6)	−179.7(3)	−179.1(4)	−176.3(3)	179.7(6)	170.9(3)	174.9(5)
φ_3							−79.6(12)	−55.4(4)	55.2(8)
ψ_3							−30.4(4)	−37.8(4)	34.6(8)
ω_3							−176.8(9)	−177.5(3)	177.7(5)
φ_4									56.8(8)
ψ_4									35.5(9)
ω_4									178.2(6)
φ_5									70.4(9)
ψ_5									15.8(10)
ω_5									175.2(8)
φ_6									−50.2(12)
"ψ_6"									−43.2(10)[a]
"ω_6"									−170.7(8)[b]

[a] N_6-C_6^{α}-C_6-O_T. [b] C_6^{α}-C_6-O_T-C_T.

tide **2** (Figure 10), which co-crystallizes with one water molecule, the N-terminal and central amino acids exhibit sets of ϕ, ψ torsion angles reasonably close to those expected for a type-II β-turn. However, a direct 1←4 intramolecular C_0=O_0···H-N_3 H-bond is not seen, as a water molecule intercalates between those two peptide functionalities with formation of a "water-bridge".[42,43] The water molecule interacts, as an acceptor, with the N_3-H group, and, as a donor, with the O_0=C_0 group. The (*S*)-Ala residue at position 3 is helical, but a second β-turn is not formed as the (*S*,*S*)-$c_3$diPhe residue at position 2 is left-handed helical, that is, of opposite handedness with respect to that of (*S*)-Ala. On the other hand, the (*S*)-(*R*,*R*)-(*S*)-tripeptide **3** (Figure 11) is highly folded in two, consecutive (slightly distorted) type-III β-turns, thus generating an incipient, right-handed 3_{10}-helical structure [thus, here too, the (*R*,*R*)-$c_3$diPhe residue is right-handed-helical]. Two 1←4 intramolecular H-bonds, C_0=O_0···H-N_3 and C_1=O_1···H-N_T, stabilize the 3D-structure of this tripeptide.

The Aib/$c_3$diPhe hexapeptide molecule **9** is found in a regular 3_{10}-helical conformation (Figure 12). In accord with the other 3D-structures described in this work, this bis(*S*,*S*)-$c_3$diPhe peptide adopts the left-handed screw sense. All four, consecutive, type-III′ β-turn forms are stabilized by 1←4 intramolecular C=O···H-N H-bonds of moderate to modest strength, the N···O separations being from 2.978(7) to 3.086(7) Å. In this hexapeptide the two $c_3$diPhe residues are positioned one on top of the other after a complete turn of the ternary helix.

As we found for the Ac_3c residues in peptides,[2,13,14] the average value for the conformationally sensitive exocyclic τ (N-C^{α}-C′) bond angle of each $c_3$diPhe residue examined is very large, 115.6±2.0°, for a regular tetrahedral value (109.5°). In each $c_3$diPhe residue there are two types of average values for the side-chain χ^1 torsion angles: $\chi^{1'}$ = ±137.0±5.8° (phenyl towards the carbonyl) and $\chi^{1''}$ = ∓6.7(8)∓5.2° (phenyl towards the nitrogen). Not surprisingly, they are quite different from that most frequently reported for the phenyl ring of Phe in peptides (g^- or −60°).[44] Interestingly, in each $c_3$diPhe residue the signs of the $\chi^{1'}$ and $\chi^{1''}$ torsion angles are opposite and strictly correlate with those of the backbone ϕ, ψ torsion angles. More specifically, $\chi^{1'}$ is positive and $\chi^{1''}$ is negative (right-handed turn/helix). As for the torsion angles relating the cyclopropane ring of each $c_3$diPhe residue to the peptide chain, N-C^{α}-C^{β}-$C^{\beta'}$ and N-C^{α}-$C^{\beta'}$-C^{β}, all sets of values observed are in the range ± 102.5–113.3°, reasonably close to the ideal *skew* (s^+, s^- or ± 120°) conformations.

Conclusion

In this work we describe the successful solution-phase synthesis of sterically hindered peptides rich in $c_3$diPhe [some of them in combination with (*S*)-Ala or Aib residues] using the step-by-step strategy. Furthermore, the results of our solution conformational analysis, taken together with those extracted from the crystal-state study, also reported here, confirm earlier preliminary findings[20,22–24,28] that $c_3$diPhe has the ability to conform well to an ideal β-turn or a $3_{10}/\alpha$-helix. This general 3D-structural tendency parallels those reported earlier for the prototypical Aib residue, Ac_3c (**I**) and other side-chain cyclized, C^{α}-tetrasubstituted α-amino acids with a larger ring size.[2,12–14]

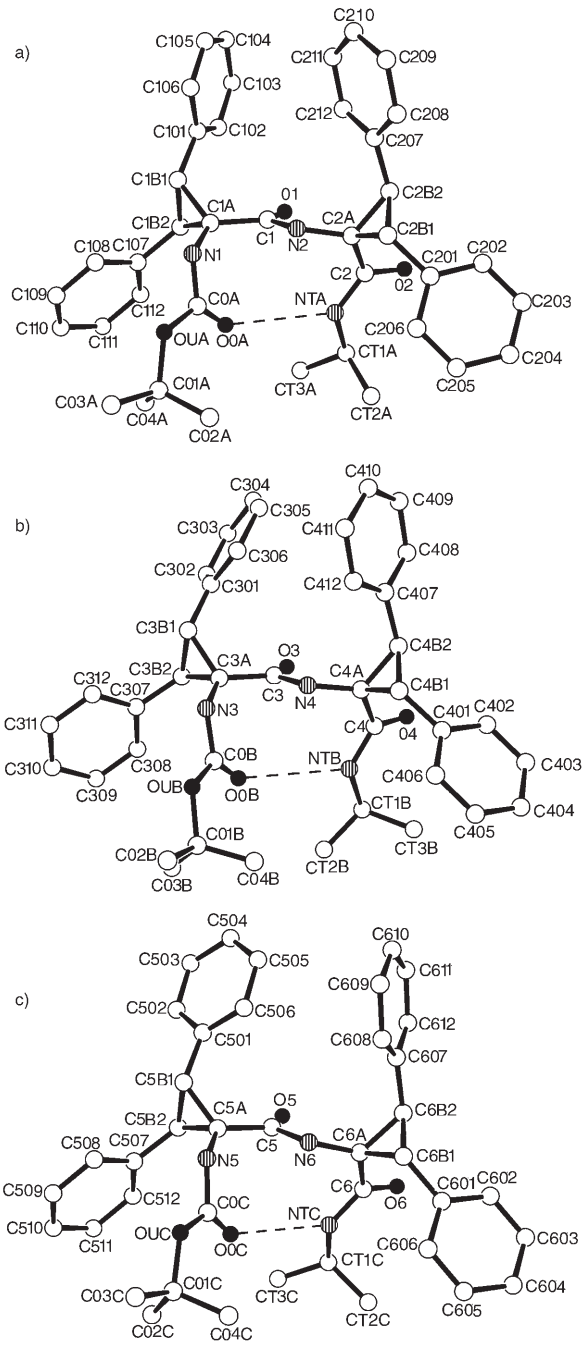

Figure 6. X-ray diffraction structures of the three independent molecules (**A**, **B**, and **C**) in the asymmetric unit of **10** with atom numbering. The intramolecular H-bond is represented by a dashed line.

As for the relationship between $c_3$diPhe chirality and the screw sense of the turn/helix that is adopted by its peptides, our NMR and X-ray diffraction data definitely support the view that the (*S*,*S*) amino acid is strongly biased in favor of the left-handedness, whereas the opposite screw sense is overwhelmingly preferred by the enantiomeric (*R*,*R*) residue, thus further authenticating the results reported by Burgess and co-workers.[28] It is worth noting that $c_3$diPhe represents one of the first amino acids investigated so far which

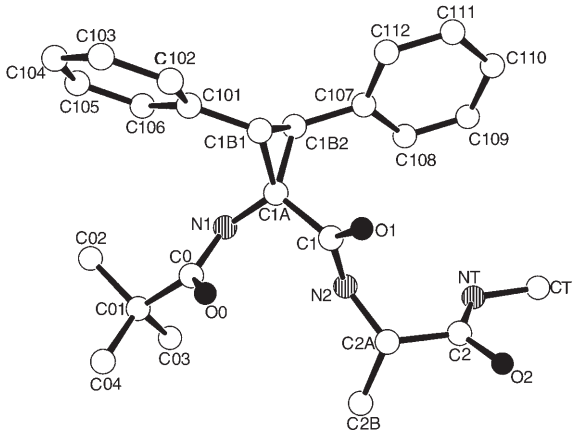

Figure 7. X-ray diffraction structure of **4** with atom numbering.

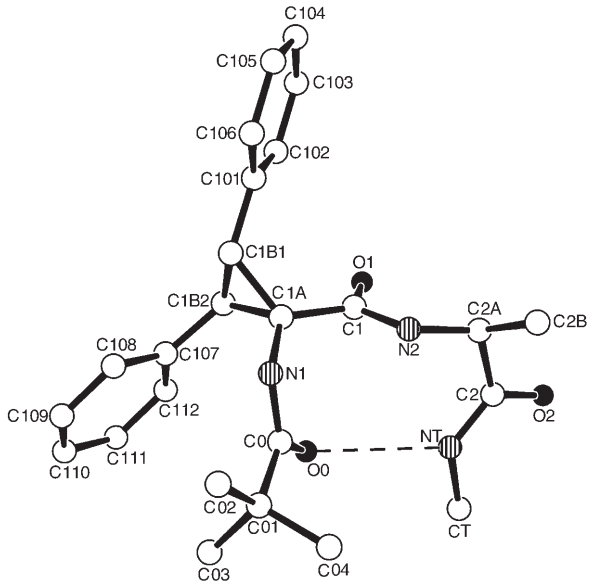

Figure 8. X-ray diffraction structure of **5** with atom numbering. The intramolecular H-bond is represented by a dashed line.

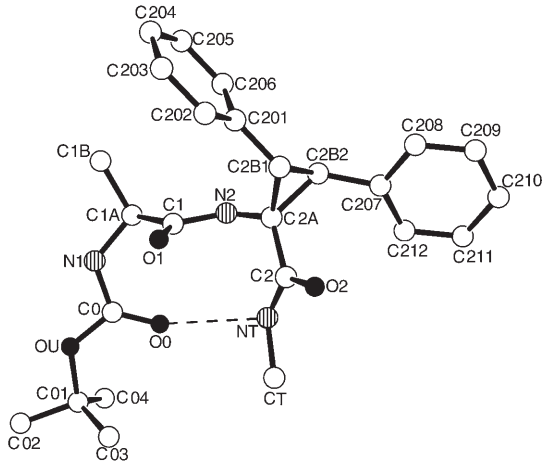

Figure 9. X-ray diffraction structure of **1** with atom numbering. The intramolecular H-bond is represented by a dashed line.

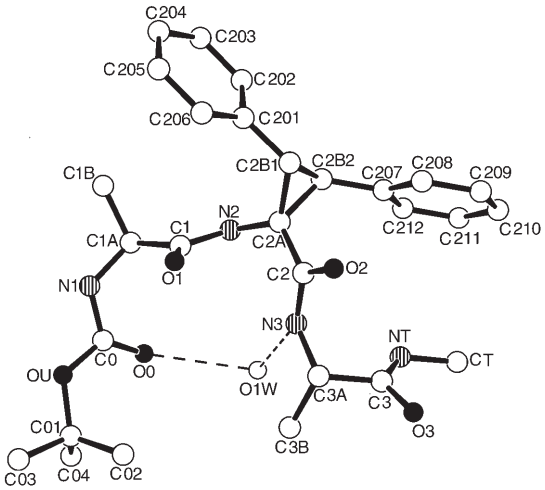

Figure 10. X-ray diffraction structure of **2** monohydrate with atom numbering. The two intramolecular H-bonds (water bridge) are represented by dashed lines.

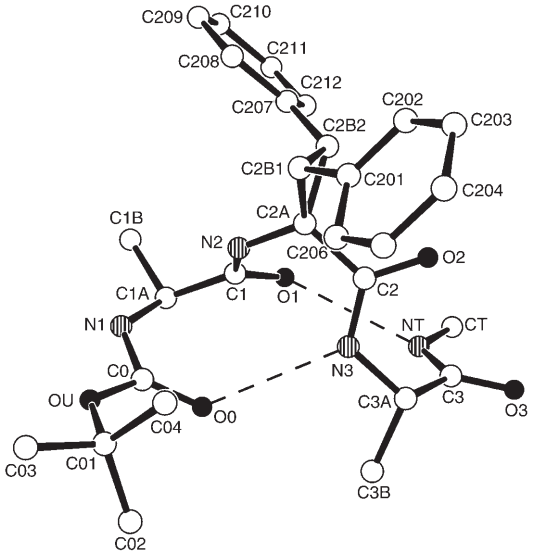

Figure 11. X-ray diffraction structure of **3** with atom numbering. The two intramolecular H-bonds are represented by dashed lines.

lacks asymmetry in the backbone (on the α-carbon atom) but possesses side-chain asymmetry (on each of the two β-carbon atoms). Previous examples include the atropoisomeric binaphthyl amino acid Bin, described by some of us (F.F. and C.T.),[45] and the side-chain bis-substituted 1-aminocyclopentane-1-carboxylic acid recently reported by Tanaka, Suemune and their co-workers,[46,47] the latter being strictly related to $c_3$diPhe as both residues are members of the class of side-chain disubstituted (on two vicinal carbons) 1-aminocycloalkane-1-carboxylic acids. It is also worth pointing out that the 3D-structural propensity of $c_3$diPhe seems to be divergent, at least in part, from that of its side-chain positional isomer 1-amino-2,2-diphenylcyclopropane-1-carboxylic acid (or α,β-methanodiphenylalanine) (**III**) in the sense that the

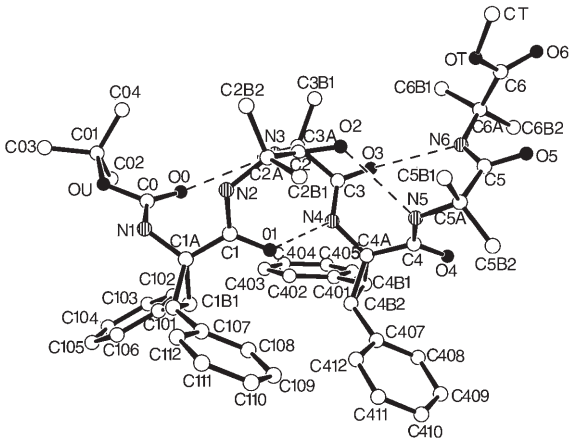

Figure 12. X-ray diffraction structure of **9** with atom numbering. The four intramolecular H-bonds are represented by dashed lines.

latter may easily explore the region of the ϕ,ψ space (−70°,70°) where the γ-turn conformation is usually found,[4,6,7] as recently demonstrated by two of us (A.I.J. and C.C.).[21]

Finally, the effect of formal side-chain cyclization upon the preferred peptide backbone 3D-structure turns out clearly from a comparison of the results of $c_3$diPhe (**IV**) discussed in this work with those already published[2] of the open-chain analogue $C^{\alpha,\alpha}$-dibenzylglycine (**V**) residue with the same number of side-chain carbon atoms: the latter is strongly biased towards the fully-extended conformation,[4,9] whereas folded structures are overwhelmingly preferred by the former. A parallel trend was already reported for other 1-aminocycloalkane-1-carboxylic acids as compared to their corresponding open-chain analogues.[2]

Experimental Section

FT-IR absorption spectroscopy: FT-IR absorption spectra were recorded in solution with a Perkin-Elmer 1720X FT-IR spectrophotometer, nitrogen flushed, with a sample-shuttle device, at 2 cm^{-1} nominal resolution, averaging 100 scans. Solvent (baseline) spectra were recorded under the same conditions. Cells with CaF_2 windows and path lengths of 0.1, 1.0 and 10 mm were used. Spectrograde $CDCl_3$ (99.8%) was obtained from Fluka.

NMR spectrometry: ^{1}H NMR spectra were recorded with a Bruker AM 400 spectrometer. Measurements were carried out in $CDCl_3$ (99.96%, Acros Organics) and [D_6]dimethylsulfoxide (99.96%, Acros Organics).

CD spectroscopy: CD spectra were recorded on a Jasco model J-715 spectropolarimeter. Fused quartz cells of 10, 1, and 0.2 mm path lengths were employed. The data are expressed in term of $[\theta]_T$, the total molar ellipticity (deg cm^2 $dmol^{-1}$). Spectrograde methanol (Fluka) was used as solvent.

X-ray-diffraction: Crystals of **10** monohydrate and diethyl ether solvate, **1**–**5**, and **9** were grown by slow evaporation from the solvents listed in the Supporting Information (Table S2). Diffraction data were collected on a Philips PW 1100 diffractometer. Crystallographic data are given in the Supporting Information (Table S2). All structures were solved by direct methods with the SIR 2002[48] program. Refinements were carried out on F^2 by the full-matrix block least-squares procedure, using all data, by application of the SHELXL 97[49] program, with all non-hydrogen

atoms anisotropic and their positional parameters and the anisotropic displacement parameters being allowed to refine at alternate cycles. The phenyl groups of all $c_3$diPhe residues were constrained to the idealized geometry. Hydrogen-atoms were calculated at idealized positions. During the refinement they were allowed to ride on their carrying atoms with U_{iso} set equal to 1.2 (or 1.5 for the methyl groups) times the U_{eq} of the parent atom.

Expected density considerations, based upon cell volume and symmetry, pointed to the likely presence of three independent peptide molecules (**A**, **B**, and **C**) in the asymmetric unit of **10**. The structure was solved by the SIR 2002 program in its default mode for medium-sized molecules by use of 2128 *E*-values >1.2. The trial solution with the best figure of merit allowed the location of all non-hydrogen atoms of the three independent peptide molecules and the co-crystallized water molecule. The positions of additional atoms, belonging to two co-crystallized diethyl ether molecules, were recovered from subsequent ΔF maps. During the refinement the displacement parameter of the atoms of one of the co-crystallized diethyl ether molecule (atoms C1Y, C2Y, O3Y, C4Y, and C5Y) leveled off to values too high to be compatible to fully occupied sites. In addition: i) some residual electron density occurs in proximity of the aforementioned atoms, and ii) there are no obvious, strong stabilizing interactions with surrounding molecules. Taken together, these observations point to the likely occurrence of some molecular disorder. On these bases, a 0.50 population parameter was imposed to all atoms of the diethyl ether molecule, although the residual electron density turned out to be too diffuse to allow a satisfactory modeling of a second conformer. Restraints were applied to the bond angles of the N- and C-terminal *t*Bu and *i*Pr groups of the three peptide molecules, as well as to the bond angles, bond angles, and the anisotropic displacement parameters of the non-hydrogen atoms of both co-crystallized diethyl ether molecules. The hydrogen atoms of the co-crystallized water molecule were located on a ΔF map and their positional parameters were not refined.

The *t*Bu group of the N-terminal Piv moiety of **4** is disordered. It was refined with the three methyl groups on two sets of positions with population parameters of 0.64 and 0.36, respectively. Restraints were applied to the bond angles involving the disordered atoms. Restraints were also imposed to the bond angles and the anisotropic displacement parameters of the C03 and C04 atoms of the N-terminal Boc group of **1**, and to the anisotropic displacement parameters of the C204, C3A, C3B, C3, and O3 atoms of **2**. In this latter structure the hydrogen atoms of the co-crystallized water molecule were located on a ΔF map and their positional parameters were not refined.

CCDC 254024 and 278785 to 278790 contain the supplementary crystallographic data for this paper. These data can be obtained free of charge from the Cambridge Crystallographic Data Centre via www.ccdc.cam.ac.uk/data request/cif/

Acknowledgements

W.M.D.B. thanks the Research-Foundation–Flanders (FWO-Vlaanderen) for his post-doctoral fellowship. Financial support from the Ministerio de Educación y Ciencia (CTQ2004-5358), DGA (predoctoral fellowship to S.R.), and CAI (travel grant to S.R.) is acknowledged.

[1] I. L. Karle, P. Balaram, *Biochemistry* **1990**, *29*, 6747–6756.
[2] C. Toniolo, M. Crisma, F. Formaggio, C. Peggion, *Biopolymers* **2001**, *60*, 396–419.
[3] C. M. Venkatachalam, *Biopolymers* **1968**, *6*, 1425–1436.
[4] C. Toniolo, *CRC Crit. Rev. Biochem.* **1980**, *9*, 1–44.
[5] G. D. Rose, L. M. Gierasch, J. A. Smith, *Adv. Protein Chem.* **1985**, *37*, 1–109.
[6] G. Némethy, M. P. Printz, *Macromolecules* **1972**, *5*, 755–758.
[7] B. W. Matthews, *Macromolecules* **1972**, *5*, 818–819.
[8] C. Toniolo, E. Benedetti, *Trends Biochem. Sci.* **1991**, *16*, 350–353.
[9] C. Toniolo, M. Crisma, F. Formaggio, C. Peggion, Q. B. Broxterman, B. Kaptein, *Biopolymers* **2004**, *76*, 162–176.
[10] S. H. Gellman, *Acc. Chem. Res.* **1998**, *31*, 173–180.
[11] C. Toniolo, M. Crisma, F. Formaggio, C. Peggion, Q. B. Broxterman, B. Kaptein, *J. Inclusion Phenom. Macrocyclic Chem.* **2005**, *51*, 121–136.
[12] M. Crisma, G. M. Bonora, C. Toniolo, V. Barone, E. Benedetti, B. Di Blasio, V. Pavone, C. Pedone, A. Santini, F. Fraternali, A. Bavoso, F. Lelj, *Int. J. Biol. Macromol.* **1989**, *11*, 345–352.
[13] E. Benedetti, B. Di Blasio, V. Pavone, C. Pedone, A. Santini, V. Barone, F. Fraternali, F. Lelj, A. Bavoso, M. Crisma, C. Toniolo, *Int. J. Biol. Macromol.* **1989**, *11*, 353–360.
[14] E. Benedetti, B. Di Blasio, V. Pavone, C. Pedone, A. Santini, M. Crisma, G. Valle, C. Toniolo, *Biopolymers* **1989**, *28*, 175–184.
[15] K. I. Varughese, C. H. Wang, H. Kimura, C. H. Stammer, *Int. J. Pept. Protein Res.* **1988**, *31*, 299–300.
[16] K. Burgess, K.-K. Ho, B. Pal, *J. Am. Chem. Soc.* **1995**, *117*, 3808–3819.
[17] A. I. Jiménez, R. Vanderesse, M. Marraud, A. Aubry, C. Cativiela, *Tetrahedron Lett.* **1997**, *38*, 7559–7562.
[18] A. I. Jiménez, C. Cativiela, A. Aubry, M. Marraud, *J. Am. Chem. Soc.* **1998**, *120*, 9452–9459.
[19] D. Moye-Sherman, M. B. Welch, J. Reibenspies, K. Burgess, *Chem. Commun.* **1998**, 2377–2378.
[20] D. Moye-Sherman, S. Jin, S. Li, M. B. Welch, J. Reibenspies, K. Burgess, *Chem. Eur. J.* **1999**, *5*, 2730–2739.
[21] A. I. Jimenez, G. Ballano, C. Cativiela, *Angew. Chem.* **2005**, *117*, 400–403; *Angew. Chem. Int. Ed.* **2005**, *44*, 396–399.
[22] A. I. Jimenez, C. Cativiela, M. Marraud, *Tetrahedron Lett.* **2000**, *41*, 5353–5356.
[23] A. I. Jiménez, P. López, L. Oliveros, C. Cativiela, *Tetrahedron* **2001**, *57*, 6019–6026.
[24] J. Casanovas, A. I. Jiménez, C. Cativiela, J. J. Pérez, C. Alemán, *J. Org. Chem.* **2003**, *68*, 7088–7091.
[25] S. S. Zimmerman, M. S. Pottle, G. Némethy, H. A. Scheraga, *Macromolecules* **1977**, *10*, 1–9.
[26] K. A. Williams, C. M. Deber, *Biochemistry* **1991**, *30*, 8919–8923.
[27] A. Yaron, F. Naider, *Crit. Rev. Biochem. Mol. Biol.* **1993**, *28*, 31–81.
[28] D. Moye-Sherman, S. Jin, I. Ham, D. Lim, J. M. Scholtz, K. Burgess, *J. Am. Chem. Soc.* **1998**, *120*, 9435–9443.
[29] S. Royo, W. M. De Borggraeve, C. Peggion, F. Formaggio, M. Crisma, A. I. Jiménez, C. Cativiela, C. Toniolo, *J. Am. Chem. Soc.* **2005**, *127*, 2036–2037.
[30] L. A. Carpino, *J. Am. Chem. Soc.* **1993**, *115*, 4397–4398.
[31] S. Mizushima, T. Shimanouchi, M. Tsuboi, R. Souda, *J. Am. Chem. Soc.* **1952**, *74*, 270–271.
[32] M. T. Cung, M. Marraud, J. Néel, *Ann. Chim.* **1972**, 183–209.
[33] M. Palumbo, S. Da Rin, G. M. Bonora, C. Toniolo, *Makromol. Chem.* **1976**, *177*, 1477–1492.
[34] C. Toniolo, G. M. Bonora, V. Barone, A. Bavoso, E. Benedetti, B. Di Blasio, P. Grimaldi, F. Lelj, V. Pavone, C. Pedone, *Macromolecules* **1985**, *18*, 895–902.
[35] J. D. Augspurger, V. A. Bindra, H. A. Scheraga, A. Kuki, *Biochemistry* **1995**, *34*, 2566–2576.
[36] K. Wüthrich, *NMR of Proteins and Nucleic Acids*, Wiley, New York, **1986**.
[37] D. Martin, H. G. Hauthal, *Dimethyl Sulphoxide*, Van Nostrand-Reinhold, Wokingham, UK, **1975**.
[38] N. S. Simmons, A. O. Barel, A. N. Glazer, *Biopolymers* **1969**, *7*, 275–279.
[39] E. Peggion, M. Palumbo, G. M. Bonora, C. Toniolo, *Bioorg. Chem.* **1974**, *3*, 125–132.
[40] IUPAC-IUB Commission on Biochemical Nomenclature, *Biochemistry* **1970**, *9*, 3471–3479.
[41] C. H. Görbitz, *Acta Crystallogr. Sect. B* **1989**, *45*, 390–395.
[42] C.-H. Yang, J. N. Brown, K. D. Kopple, *Int. J. Pept. Protein Res.* **1979**, *14*, 12–20.
[43] N. Thanki, Y. Umrania, J. M. Thornton, J. M. Goodfellow, *J. Mol. Biol.* **1991**, *221*, 669–691.

[44] E. Benedetti, G. Morelli, G. Némethy, H. A. Scheraga, *Int. J. Pept. Protein Res.* **1983**, *22*, 1–15.
[45] J.-P. Mazaleyrat, K. Wright, A. Gaucher, M. Wakselman, S. Oancea, F. Formaggio, C. Toniolo, V. Setnicka, J. Kapitán, T. A. Keiderling, *Tetrahedron: Asymmetry* **2003**, *14*, 1879–1893.
[46] M. Tanaka, Y. Demizu, M. Doi, M. Kurihara, H. Suemune, *Angew. Chem.* **2004**, *116*, 5474–5477; *Angew. Chem. Int. Ed.* **2004**, *43*, 5360–5363.
[47] M. Tanaka, K. Anan, Y. Demizu, M. Kurihara, M. Doi, H. Suemune, *J. Am. Chem. Soc.* **2005**, *127*, 11570–11571.
[48] M. C. Burla, M. Camalli, B. Carrozzini, G. L. Cascarano, C. Giacovazzo, G. Polidori, R. Spagna, *J. Appl. Crystallogr.* **2003**, *36*, 1103.
[49] G. M. Sheldrick, *SHELXL 97. Program for the Refinement of Crystal Structures*, University of Göttingen, Göttingen, Germany, **1997**.

Received: July 22, 2005
Published online: November 10, 2005

